The Effect of Diabetic Medicine Exendin-4 on Lipopolysaccharide-induced Bone Resorption, Osteoclast Formation, and Orthodontic Tooth Movement

博 士 論 文

The Effect of Diabetic Medicine Exendin-4 on Lipopolysaccharide-induced Bone Resorption, Osteoclast Formation, and Orthodontic Tooth Movement

（糖尿病治療薬exendin-4のlipopolysaccharideによる破骨細胞形成および骨吸収と矯正的歯の移動への影響）

沈　威任

令和二年度提出

東北大学

Contents

1. Abstract

Glucagon-like peptide-1 (GLP-1) receptor agonists are an effective treatment approach for type 2 diabetes. Recently, anti-inflammatory effects of GLP-1 receptor agonists have also been reported. Lipopolysaccharide (LPS) induces inflammation and osteoclast formation. At first, we investigated the effect of exendin-4, a widely used GLP-1 receptor agonist, in LPS-induced osteoclast formation and bone resorption. LPS with or without exendin-4 was administered on mouse calvariae by daily subcutaneous injection. The number of osteoclasts ($p<0.01$), the ratio of bone resorption pits ($p<0.05$) and the level of C-terminal cross-linked telopeptide of type I collagen (CTX) ($p<0.01$) were significantly lower in LPS and exendin-4 co-administered mice than in mice administered LPS alone. RANKL ($p<0.05$) and TNF-α ($p<0.01$) mRNA expression levels were lower in the exendin-4 and LPS co-administered group than in the LPS-administered group. Our *in vitro* results showed no direct effects of

exendin-4 on RANKL-induced osteoclast formation, TNF-α-induced osteoclast formation, or LPS-induced RANKL expression in stromal cells. Conversely, TNF-α mRNA expression was inhibited in the exendin-4 and LPS co-treated macrophages compared with cells treated with LPS alone ($p<0.01$). These results indicate that the GLP-1 receptor agonist exendin-4 may inhibit LPS-induced osteoclast formation and bone resorption by inhibiting LPS-induced TNF-α production in macrophages.

Orthodontic patients with diabetes mellitus are increasing due to global population aging and poor dietary management, so it is crucial to understand the effect of diabetes medicine on orthodontic tooth movement. Exendin-4, a GLP-1 receptor agonist, is a subcutaneously administered medicine for type II diabetic patients with less side effects. The second purpose of this study was to investigate the effects of exendin-4 on orthodontic tooth movement distance, root resorption and expressions of osteoclast-related cytokines.

A 10 gm NiTi coil spring was placed between the anterior alveolar bone and upper left first molar of each eight-week-old male C57BL/6 mouse. 20 μl exendin-4 solutions (containing 0.2 μg, 4 μg or 20 μg exendin-4) or PBS solution was injected on the buccal side of upper left first molar respectively every two days (n=4). After sacrifice on twelfth day, silicone impressions were taken to record tooth movement distance. 20 μg exendin-4 injection group had lower orthodontic tooth movement distance than PBS injection group ($p<0.01$). The left maxillae of PBS and 20 μg exendin-4 injection groups were also excised for histological analysis and RT-PCR analysis. Compared to PBS group, 20 μg exendin-4 injection group showed lower osteoclast number ($p<0.05$), and odontoclast number ($p<0.05$), and root resorption surface percentage ($p<0.05$). The maxillae with 20 μg exendin-4 injections also had lower RANKL mRNA expression ($p<0.05$), TNF-α mRNA expression ($p<0.05$), and RANKL/OPG ratio ($p<0.01$) than the maxillae with PBS injections. There was no difference in

the expression of OPG mRNA.

Exendin-4 inhibits orthodontic tooth movement, so more attention should be paid to orthodontic patients who take exendin-4 for diabetes treatment. Since exendin-4 prevents orthodontic root resorption, GLP-1 receptor may be a treatment target for clinical cases with severe root resorption.

2. Introduction

Patients with type II diabetes is increasing worldwide, accounting for 8.5 % of the adult population (18 years and older) (WHO world report. 2016). Glucagon-like peptide-1 (GLP-1) receptor agonists, which resemble the intestinal GLP-1 hormone but have more resistance to the degradation of dipeptidyl peptidase-IV (DPP-4), have been developed to treat type 2 diabetes (Garber et al. 2011). They function by preventing the apoptosis, increasing the sensitivity, and stimulating insulin release of pancreatic β cells (Arakawa et al. 2009, Drucker 2003, Wei et al. 2012). Because of wide expression of GLP-1 receptors in various cell types (Körner et al. 2007), supplemental effects in addition to blood glucose control have been investigated recently. As shown in many animal studies, GLP-1 receptor agonists are also able to suppress chronic inflammation of different organs through down-regulating the expression of inflammatory cytokines, including IL-1, IL-6, and TNF-α (Lee et al. 2016).

Individuals with type 2 diabetes have been shown to have a higher risk of bone fracture compared with individuals without type 2 diabetes (Moayeri et al. 2017). This higher risk might be associated with the pathobiology of type 2 diabetes itself; however, the underlying mechanisms remain unclear (Walsh et al. 2017). Additionally, increased bone fracture risk is a consequence of therapeutic regimen used to treat hyperglycemia (Montagnani et al. 2013). For example, patients treated with thiazolidinediones and human recombinant insulin have been shown to have an increased bone fracture risk (Bazelier et al. 2012, Betteridge et al. 2011, Schwartz et al. 2011). Conversely, treatment with metformin is related to decreased bone fracture risk (Vestergaard et al. 2005). Recent meta-analyses have reported that GLP-1 receptor agonist treatment does not affect fracture risk in type 2 diabetic patients (Mabilleau et al. 2014, Nuche-Berenguer et al. 2009).

Osteoclast recruitment is crucial to the pathogenesis of diseases

involving bone erosion, such as rheumatoid arthritis (Redlich et al. 2002). Osteoclasts derived from bone marrow cells are responsible for bone resorption and remodeling (Teitelbaum 2000). Receptor activator of NF-kB ligand (RANKL) and macrophage colony stimulating factor (M-CSF) are two key factors required for osteoclast formation and activation (Teitelbaum 2007). Independent of RANKL, tumor necrosis factor (TNF)-α has also been reported to induce osteoclast formation *in vitro* (Azuma et al. 2000, Kobayashi et al. 2000, Fuller et al. 2002) and *in vivo* (Kitaura et al. 2004, Kitaura et al. 2005).

Lipopolysaccharide (LPS) strongly induces inflammation and inflammatory bone loss (Orcel et al. 1993, Abu-Amer et al. 1997, Sakuma et al. 2000, Dumitrescu et al. 2004, Chung et al. 2006). LPS has also been found to induce production of pro-inflammatory cytokines, such as TNF-α, from macrophages or other cells at the site of inflammation (Bostanci et al. 2007, Kitaura et al. 2013). Such pro-inflammatory cytokines have been

reported to be involved in LPS-induced osteoclast formation and bone destruction in *in vivo* and *in vitro* studies (Abu-Amer et al. 1997, Chiang et al. 1999, Zou et al. 2002, Garlet et al. 2006, Mormann et al. 2008). Additionally, LPS can stimulate osteoblasts to produce or secrete RANKL (Kikuchi et al. 2001).

GLP-1 receptor-deficient mice were reported to exhibit osteopenia and increased osteoclast formation, suggesting that the GLP-1 signaling has an inhibitory effect of bone resorption on bone metabolism (Yamada et al. 2008). An anabolic effect of GLP-1 on bone metabolism has also been proposed. GLP-1 receptors activation has been shown to induce bone formation in streptozotocin-induced diabetic and fructose-stimulated insulin-resistant rats (Nuche-Berenguer et al. 2010).

The anabolic and antiresorptive effects of GLP-1 receptor suggest that GLP-1 receptor signaling may be a promising therapeutic target for osteoporosis or other osteolytic bone diseases; such a therapeutic approach

would be facilitated by the fact that the first commercially available GLP-1 receptor agonist, exendin-4, has already been approved for the treatment of diabetes for over 10 years (Brubaker 2007). Now it is still administered by subcutaneous injections. Exendin-4 shares similar structural and functional properties to GLP-1, but it resistant to the degradation by DPP-4, which can degrade GLP-1 immediately in the blood (Meier et al. 2004). The extended half-life, improved pharmacokinetics, and high potency of exendin-4 make it suitable for clinical use (Meier et al. 2004, Nielsen et al. 2003, Ma et al. 2013). Exendin-4 is reported to be the most potent GLP-1 receptor agonist that can reduce bone fracture rate of diabetic patients (Zhang et al. 2018).

Therefore, we investigated the effects of exendin-4 on LPS-induced osteoclast formation and bone remodeling in mice.

Orthodontic tooth movement is a dynamic process achieved by bone resorption by osteoclasts on the compression side and bone apposition by

osteoblasts on the tension side. During this process, root resorbing odontoclasts also appears along with osteoclasts. The receptor activator of nuclear factor kappa-B ligand (RANKL) (Yang et al. 2018, Tyrovola et al. 2008) and tumor necrosis factor-α (TNF-α) (Kitaura et al. 2008, Ogawa et al. 2019) are crucial in the differentiation of osteoclasts and odontoclasts during orthodontic tooth movement. On the other hand, exendin-4 is capable of reducing not only TNF-α expression (Arakawa et al. 2010, Shen et al. 2018) but also TNF-α-induced inflammation or reactions (Dorecka et al. 2013, Garczorz et al. 2018, Cao et al. 2015). Increased RANKL expression in the bone of osteoporotic rodents are also ameliorated by exendin-4 administrations (Nuche-Berenguer et al. 2009, Nuche-Berenguer et al. 2011, Ma et al. 2013). Therefore, the present study is to ascertain the effects of exendin-4 on orthodontic tooth movement and associated root resorption in a mouse model.

3. Materials and methods

Animals and reagents

Eight- to ten-week-old male C57BL6/J mice were obtained from CLEA Japan (Tokyo, Japan) and maintained at our animal facility. All animal care and experiments were conducted according to Tohoku University rules and regulations. Four mice were randomly assigned to each experimental group. Both *Escherichia coli* LPS and exendin-4 were purchased from Sigma-Aldrich (St. Louis, MO).

Histological analysis for LPS-induced bone resorption

A previous *in vivo* study demonstrated that daily subcutaneous injections of 100 μg LPS to mouse calvariae for 5 days effectively induced osteoclast formation (Kimura et al. 2012). Therefore, we followed the same protocol, dose, and LPS administration period in this study. The mice were divided

into four experimental groups and subjected to daily subcutaneous injections on the calvaria with phosphate-buffered saline (PBS, negative control group), LPS alone (100 μg/day, positive control group), LPS (100 μg/day) and exendin-4 (20 μg/day), and exendin-4 alone (20 μg/day) for 5 days. All mice calvariae were excised immediately after sacrifice on the sixth day. The calvariae were fixed in 4% PBS-buffered formaldehyde at 4°C overnight and the demineralized with 14% ethylenediaminetetraacetic acid (EDTA) at room temperature for three days. Each calvaria was cut into three pieces perpendicular to the sagittal suture. Samples were then embedded in paraffin and cut into 5-μm sections using a microtome. The paraffin sections were stained with tartrate-resistant acid phosphatase (TRAP) solution prepared by mixing acetate buffer (pH 5.0), naphthol AS-MX phosphate (Sigma Chemical, St. Louis, MO, USA), Fast Red Violet LB salt (Sigma), and 50 mM sodium tartrate. The sections were counterstained with hematoxylin. Osteoclasts were defined in this study as

TRAP-positive cells with three or more nuclei. We counted the number of osteoclasts only at the suture mesenchyme of the sagittal suture in all slides according to the method in our previous work (Saeed et al. 2016).

Preparation of osteoclast precursors for osteoclastogenesis

To isolate bone marrow cells from C57BL6/J mice, femora and tibiae were aseptically removed after sacrifice. The epiphyses of these long bones were removed and the bone marrow was flushed into a sterile Petri dish with a 25-gauge needle and 10-ml syringe filled with culture medium. The bone marrow was then filtered with a 40-μm nylon cell strainer (Falcon, USA) and centrifuged. The harvested cells were incubated in a culture medium comprising alpha-modified minimal essential medium (α-MEM; Sigma) containing 10% fetal bovine serum (FBS), 100 IU/ml penicillin G (Meiji Seika, Tokyo, Japan), and 100 μg/ml streptomycin (Meiji Seika), with M-CSF added. Non-adherent cells were removed by washing with

PBS, and adherent cells were harvested using trypsin-EDTA solution (Sigma Aldrich). The harvested cells were seeded and further cultured in the presence of M-CSF. Adherent cells were used as osteoclast precursors in this study (Saeed et al. 2016). Osteoclast precursors were seeded at 5×10^4 cells per 200 μl of medium in a 96-well plate and cultured in medium containing M-CSF alone (100 ng/ml), M-CSF (100 ng/ml) and RANKL (100 ng/ml) or TNF-α (100 ng/ml), M-CSF (100 ng/ml) and RANKL (100 ng/ml) or TNF-α (100 ng/ml) with exendin-4 (100 ng/ml), and M-CSF (100 ng/ml) with exendin-4 (100 ng/ml), for 5 days. The cultured cells were then fixed with 10% formalin for 30 min. After fixation, the cells were permeabilized with 0.2% Triton X-100 for 5 min at room temperature, then incubated in TRAP staining solution prepared as described above. TRAP-positive cells with three or more nuclei were considered to be osteoclasts and were counted under a light microscope.

Preparation of bone marrow stromal cells

Bone marrow cells were obtained by the method described above and cultured in Dulbecco's modified Eagle's medium (D-MEM; Sigma) containing 10% FBS, 100 IU/ml penicillin G (Life Technology, Carlsbad, CA) and 100 μg/ml streptomycin (Life Technology) for two weeks. Then the culture disks were washed vigorously with PBS to remove non-adherent cells. Adherent cells were used as stromal cells in this study (Saeed et al. 2016).

Isolation of murine macrophages

Macrophages were obtained from the peritoneal cavity of mice. To obtain resident macrophages under resting conditions, we injected 5 ml of sterile ice-cold PBS (pH 7.4) into the peritoneal cavity and aspirated the fluid to harvest peritoneal cells. The cell were washed twice with α-MEM medium (Sigma) containing 10% FBS. After 1 hour of culture,

non-adherent cells were removed; and after 24 hours of culture, adherent cells were harvested and used as macrophages.

Isolation of RNA and real-time RT-PCR analysis

Calvariae from the *in vivo* experiments were frozen in liquid nitrogen and crushed by Micro Smash MS-100R (Tomy Seiko, Tokyo, Japan) in 800 μl TRIzol reagent (Invitrogen, Carlsbad, CA) for each sample. Total RNA was extracted with an RNeasy mini kit (Qiagen, Valencia, CA) according to the manufacturer's protocol. For the *in vitro* experiments, bone marrow stromal cells or macrophages were incubated in culture medium supplemented with PBS, LPS (100 ng/ml), LPS (100 ng/ml) and exendin-4 (100 ng/ml), and exendin-4 (100 ng/ml). After three days of culture, total RNA was isolated from adherent cells. Total RNA of stromal cells or peritoneal macrophages was isolated using an RNeasy mini kit (Qiagen). cDNA was synthesized for each sample from 2 μg total RNA

with oligo-dT primers (Invitrogen) and reverse transcriptase in a total volume of 20 μl. The corresponding expression levels of RANKL and TNF-α mRNA were evaluated by real-time RT-PCR using a Thermal Cycler Dice Real Time system (Takara, Shiga, Japan). Each reaction comprised a total volume of 25 μl containing 2 μl cDNA and 23 μl of a mixture of SYBR Premix Ex Taq (Takara) and 50 pmol/μl primers. The PCR cycling conditions were as follows: 95 °C for 10 s for initial denaturation followed by 45–60 amplification cycles, with each cycle comprising a denaturation step of 95 °C for 5 s and then an annealing step of 60 °C for 30 s. Relative expression levels of TNF-α and RANKL mRNAs were calculated by normalization to glyceraldehyde 3-phosphate dehydrogenase (GAPDH) mRNA levels. The primer sequences used for cDNA amplification were as follows: 5′-GGTGGAGCCAAAAGGGTCA-3′ and 5′-GGGGGCTAAGCAGTTGGT-3′ for GAPDH; 5′-

AGGCGGTGCTTGTTCCTCA-3′ and 5′-AGGCGAGAAGATGATCTGACTGCC-3′ for TNF-α; and 5′-CCTGAGGCCAGCCATTT-3′ and 5′-CTTGGCCCAGCCTCGAT-3′ for RANKL (Saeed et al. 2016); 5′- AGGCGGTGCTTGTTCCTCA-3′ and 5′-AGGCGAGAAGATGATCTGACTGCC-3′ for TNF-α; 5′-ATCAGAGCCTCATCACTT-3′ and 5′-CTTAGGTCCAACTACAGAGGAAC-3′ for osteoprotegerin (OPG).

Micro-CT imaging and analysis for bone destruction area

We obtained mouse calvariae immediately after sacrifice. The calvariae were fixed in 4% PBS-buffered formaldehyde at 4°C for 3 days. To assess the bone resorption pits on the calvariae, samples were washed thoroughly with PBS and scanned with microfocus computed tomography (ScanXmate-E090, Comscan, Kanagawa, Japan). TRI/3D-BON64 software (RATOC System Engineering, Tokyo, Japan) was used to create

three-dimensional images of the mouse calvariae, and the ratio of bone resorption area to total area was measured by Image J (NIH, Bethesda, MD) (Saeed et al. 2016).

Measurement of serum CTX (C-terminal cross-linked telopeptide of type I collagen) value

Blood was collected with microhematocrit tubes from the orbital sinuses of the mice after 5 days of daily administration of PBS, LPS with or without exendin-4, or exendin-4 alone. The levels of CTX were determined using a mouse C-terminal telopeptide of type I collagen assay kit (IDS, Tyne and Wear, UK). Levels of C-terminal telopeptide of type I collagen were assessed by measuring absorbance at 450 nm with a microplate reader (Remote Sunrise; Tecan, Japan), with 620nm as the reference wavelength.

Cell viability assay for osteoclast precursors

Osteoclast precursors were seeded in a 96-well plate (1×10^4 cells in 200 μl medium per well) and incubated with M-CSF (100 ng/ml) with or without exendin-4 (100 ng/ml). After 5 days of incubation, the cells were washed with PBS and cultured in 100 μl culture medium of each well. Four replicates were assessed for each sample. Then, 10 μl cell counting kit-8 (Dojin, Kumamoto, Japan) solution was added to each well and the plate was further incubated for 2 h at 37°C. Absorbance at 450 nm was measured by a microplate reader for each well (Saeed et al. 2016).

Orthodontic tooth movement

For local injections, different amounts of exendin-4 were dissolved by phosphate buffered saline (PBS) according to the required doses. Orthodontic force was exerted by a 10 gm closed nickel-titanium (NiTi) spring tied between upper left first molar and anterior alveolar bone after

anesthesia of mice (Figure 6A). A 0.1 mm ligature wire was threaded through the gingival embrasure between upper left first and second molars, and tied to one end of the spring. Then, another ligature wire was threaded through a hole drilled on the anterior maxilla near the central incisors by a small round bur, and was tied to the other end of the spring. 20 μl exendin-4 solution (0.2, 4, 20 μg dissolved in 20 μl PBS solution) or PBS solution was injected on the buccal side of upper left first molar on day 0, day 2, day 4, day 6, day 8, and day 10 (n=4). For easier ingestion of food, mice were fed with powder diet (CLEA, Japan). After sacrifice on twelfth day, hydrophilic polysiloxane impressions (Examixfine®, GC, Japan) were made to measure the tooth movement distance. The distance between the distal marginal ridge of the first molar and mesial marginal ridge of the second molar on the line connecting the central fossae of the first and second molars was measured (Figure 1B) by a dissecting microscope (Leica M165FC, Germany). Then, maxillae were taken for histological

sections and real-time polymerase chain reaction (RT-PCR) analysis.

Histological quantification of osteoclasts in orthodontic tooth movement

Maxillae were fixed in 4% PBS-buffered formaldehyde at 4°C overnight and decalcified with *OSTEOSOFT*® solution (Sigma-Aldrich) at room temperature for one month. Samples were processed by tissue processer (Leica TP1020, Germany), and then embedded in paraffin. Horizontal sections that are 100, 140, 180, 220, and 260 μm apical to the bifurcation area of upper left first molar were cut. The paraffin sections with the thickness of 5 μm were then deparaffinized by xylene, hydrated with graded alcohols, and stained with tartrate-resistant acid phosphatase (TRAP) solution prepared by mixing acetate buffer (pH 5.0), naphthol AS-MX phosphate (Sigma Chemical, St. Louis, MO, USA), Fast Red Violet LB Salt (Sigma), and 50 mM sodium tartrate. Counterstaining was performed by hematoxylin. Sections were viewed by light microscopy. A

labiolingual long axis of the distobuccal root of upper left first molar was drawn, and the area mesial to this axis was considered as compression side of orthodontic tooth movement. The number of TRAP-positive osteoclasts with three or more nuclei on the alveolar surface of the compression side was counted.

Histological quantification of odontoclasts and root resorption in orthodontic tooth movement

Horizontal paraffin sections were obtained by the same method as mentioned previously. Number of TRAP-positive odontoclasts on the distobuccal root surface of upper left first molar on the compression side was measured. Thinning or lacunae of cementum with overlying odontoclasts was considered as resorptive root surface. The length of whole root surface and resorptive surface on the compression side were measured by the software Image J (National Institutes of Health, Bethesda,

Maryland, USA). Root resorption surface percentage (%) was calculated by dividing the length of whole root surface by the length of resorption surface.

Statistical analysis

All data was expressed as mean ± standard deviation. Comparisons between two groups were performed by student's t tests. Comparisons for more than three groups were done by analyses of variance (ANOVA) and post hoc Scheffe's tests. P values less than 0.05 were considered statistically significant. All statistical analyses were conducted with SPSS software (IBM, USA).

4. Results

In vivo *inhibitory effect of exendin-4 on LPS-induced osteoclast formation*

We injected LPS with or without exendin-4 on mouse calvariae to analyze the effect of exendin-4 on LPS-induced osteoclast formation *in vivo*. After LPS administration for 5 consecutive days, many large multinucleated osteoclasts were observed within the suture mesenchyme in the histological sections. However, the mean number of osteoclasts was significantly lower in the LPS and exendin-4 co-administered group than in the group administered LPS alone (Fig. 6A and 6B).

In vivo *inhibitory effect of exendin-4 on LPS-induced bone resorption*

The mouse calvariae were scanned with microfocus computed tomography and the amount of bone resorption areas was compared between each group. Many bone destruction defects were noted in the LPS

group. The ratio of the bone resorption area to the total area was significantly higher in the LPS-administered group than the PBS-administered and exendin-4-administered groups. Moreover, the LPS and exendin-4 co-administered groups demonstrated less bone destruction than the group administered LPS alone (Fig. 2A and B). Serum levels of C-terminal telopeptide of type I collagen (CTX), a marker of bone resorption, in mouse serum samples were analyzed by a mouse CTX assay kit. The serum CTX level in the LPS alone administered group was higher than PBS-administered group. However, the serum CTX level in the LPS and exendin-4 co-administered group was lower than the LPS alone administered group (Fig. 2C).

In vivo *inhibitory effect of exendin-4 on the expression of LPS-induced osteoclast related cytokines (TNF-α and RANKL).*

Bone chips from mouse calvariae were analyzed by real-time RT-PCR to

measure expression levels of TNF-α and RANKL mRNA. TNF-α and RANKL mRNA levels were elevated in the LPS-administered group compared with the PBS-administered group. Conversely, TNF-α and RANKL mRNA expression levels were reduced in the exendin-4 and LPS co-administered group compared with the LPS-administered group (Fig. 3).

Exendin-4 cannot affect RANKL-induced osteoclast formation, TNF-α-induced osteoclast formation, cell viability of osteoclast precursor cells, and LPS-induced RANKL expression in stromal cells.

To investigate whether exendin-4 affects osteoclast precursor cells directly, we analyzed the effects of exendin-4 on RANKL-induced osteoclast formation, TNF-α-induced osteoclast formation, and viability of osteoclast precursors. There were large numbers of TRAP-positive cells among osteoclast precursor cells cultured with M-CSF and RANKL or TNF-α. Likewise, TRAP-positive cells were also observed among the

osteoclast precursor cells cultured with M-CSF and RANKL or TNF-α in the presence of exendin-4 (Fig 4A and B). Additionally, there was no evident difference in cell viability between the two cultures after 5 days of culture (Fig 4C). These results indicate that the inhibitory effect of exendin-4 may be not related to a direct action of exendin-4 on the proliferation and differentiation of osteoclast precursors.

We next evaluated whether exendin-4 inhibited LPS-induced RANKL expression in stromal cells *in vitro*. RANKL mRNA expression levels were higher in LPS-treated stromal cells than in control and exendin-4-treated stromal cells. However, stromal cells treated with both LPS and exendin-4 demonstrated similar RANKL mRNA expression levels to those treated with LPS alone (Fig 4D). These results show that the inhibitory effect of exendin-4 may be not related to a direct action of exendin-4 on RANKL expression in stromal cells.

Exendin-4 suppresses LPS-induced TNF-α expression in macrophages

Real-time RT-PCR was performed to analyze TNF-α mRNA expression levels. TNF-α mRNA expression was elevated in macrophages treated with LPS alone compared with those treated with PBS. Conversely, TNF-α mRNA expression was inhibited in the exendin-4- and LPS-treated macrophages, compared with those treated with LPS alone (Fig. 5).

High-dose exendin-4 inhibited orthodontic tooth movement

After twelve days of orthodontic tooth movement, the mean tooth movement distance for PBS group was 184.5 ± 8.7 μm. For 0.2 μg, 4 μg, and 20 μg exendin-4 injection groups, the mean distances of tooth movement were 179.25 ± 11.2 μm, 163.3 ± 13.1 μm, and 137.8 ± 6.2 μm, respectively. 20 μg exendin-4 injection group had significantly lower tooth movement distance than PBS injection group (25.3% reduction, $p<0.01$). However, there was no statistical significance between PBS group, 0.2 μg

exendin-4 injection group, and 4 μg exendin-4 injection group. (Figure 6C)

Exendin-4 inhibited osteoclast formation on the compression side during orthodontic tooth movement

The mean numbers of large TRAP positive osteoclasts of PBS and exendin-4 20 μg injection groups were 12.1± 3.2 and 7.5 ± 2.3. 20 μg exendin-4 injection group exhibited lower osteoclast number on the compression side than that of PBS injection group (38.1 % reduction, $p<0.05$) (Figure 7).

Exendin-4 inhibited odontoclast formation and root resorption surface percentage on the compression side during orthodontic tooth movement

PBS injections group had severe root resorption as demonstrated by high odontoclast number (3.0 ± 1.7) and root resorption surface percentage (19.8 ± 8.8%). Mice injected with 20 μg exendin-4 had lower odontoclast

number (0.9 ± 0.8, 71.2 % reduction, $p<0.05$) (Figure 8A) and root resorption surface percentage (5.9 ± 4.2 %, 70 %reduction, $p< 0.05$) (Figure 8B) than those injected PBS.

Exendin-4 reduced expressions of RANKL and TNF-α mRNA and RANKL/OPG ratio in the maxillae with orthodontic loading

The maxillae with 20 μg exendin-4 injections had lower RANKL mRNA expression (66.3% reduction, $p< 0.05$) (Figure 9A) and TNF-αmRNA expression (45.5% reduction, $p<0.05$) (Figure 9B) than the maxillae with PBS injections during orthodontic tooth movement. Although there was no difference in the expression of OPG mRNA (Figure 9C), RANKL/OPG ratio (72.9% reduction, $p< 0.01$) (Figure 9D) was still reduced in exendin-4 group.

5. Discussion

At first, we evaluated the effect of the GLP-1 receptor agonist exendin-4 on LPS-induced osteoclast formation and bone-resorption *in vivo*. We found that the GLP-1 receptor agonist inhibited LPS-induced osteoclast formation and bone resorption, and also suppressed LPS-induced RANKL and TNF-α expression *in vivo*. Conversely, the GLP-1 receptor agonist did not directly inhibit RANKL-induced osteoclast formation, TNF-α-induced osteoclast formation, osteoclast precursor cell viability, or LPS-induced RANKL expression in stromal cells *in vitro*. However, the GLP-1 receptor agonist inhibited LPS-induced TNF-α expression in macrophages *in vitro*.

GLP-1 plays a crucial role in blood glucose control. To simulate the effect of GLP-1, many GLP-1 analogues and GLP-1 receptor agonists have been developed. The amino acid sequence of the GLP-1 receptor agonist exendin-4 is a modified version of the sequence of GLP-1. Exendin-4 is resistant to degradation by dipeptidyl peptidase-IV and has a much longer

plasma half-life than GLP-1 (Nielsen et al. 2003), which has a half-life of less than two minutes (Meier et al. 2004, Ma et al. 2013). The extended half-life, improved pharmacokinetics, and high potency of exendin-4 make it suitable for clinical use (Meier et al. 2004, Nielsen et al. 2003).

In this study, we administered 20μg/day exendin-4 for 5 days, injected into the supracalvaria. Although previous rodent studies used 20μg/kg exendin-4 daily for 4 weeks (Ma et al. 2013, Pereira et al. 2015), we opted to use a higher dose to enhance the inhibitory effects of exendin-4. Further investigation using clinically relevant doses is needed.

Our findings prompted us to explore the mechanisms contributing to the inhibition of LPS-induced osteoclast formation and bone resorption. We considered two possible mechanisms. First, we considered whether exendin-4 inhibited LPS-induced expression of inflammatory cytokines related to osteoclast formation, such as TNF-α and RANKL. Many studies have indicated that LPS induces TNF-α and RANKL *in vivo* (Kikuchi et al.

2001, Wada et al. 2004). RANKL is an essential cytokine for osteoclast formation (Teitelbaum, 2000), and it has been reported that TNF-α also can induce osteoclast formation *in vivo* (kitaura et al. 2004, kitaura et al. 2005). Therefore, it is reasonable to suspect that if levels of both of these cytokines are decreased, osteoclast formation will be inhibited. In the present study, TNF-α and RANKL mRNA levels were elevated in the LPS-administered mice. However, this LPS-induced increase in TNF-α and RANKL mRNA levels was inhibited in the exendin-4 and LPS co-administered group, compared with the group administered LPS only. This suggests that one of the mechanisms underlying the inhibitory effect of exendin-4 on LPS-induced osteoclast formation is the inhibition of LPS-induced osteoclast-related cytokines. The other mechanism that we considered was that exendin-4 directly inhibited RANKL- and TNF-α-induced osteoclast formation. In the present study, we investigated whether exendin-4 exerted its inhibitory effect on osteoclasts by directly

acting on osteoclast precursors. However, exendin-4 did not inhibit RANKL- or TNF-α-induced differentiation of osteoclast precursor cells into osteoclasts. Moreover, we investigated whether exendin-4 inhibited osteoclast precursor cell viability. We observed no difference in cell viability between the two groups after 5 days of culture. These results suggest that the inhibitory effect of exendin-4 on osteoclast formation is not due to a direct action of exendin-4 on osteoclast precursors. We then evaluated whether exendin-4 inhibited LPS-induced RANKL expression in stromal cells. Exendin-4 also failed to inhibit LPS-induced RANKL expression in stromal cells. This indicates that inhibition of RANKL expression by exendin-4 may not be due to a direct action of exendin-4 on stromal cells. Finally, we evaluated whether exendin-4 inhibited LPS-induced TNF-α expression in macrophages. In our study, exendin-4 inhibited LPS-induced TNF-α expression of macrophages. GLP-1 receptor is a G protein-coupled receptor that can activate adenylate cyclase to

produce cAMP on activation. In macrophages, cAMP/PKA pathway suppresses the production of pro-inflammatory cytokines (Aronoff et al. 2005). Exendin-4 was reportedly able to reduce LPS-induced macrophage activation and TNF-α expression through PKA/NF-κB signaling pathway (Arakawa et al. 2010). Exendin-4 can also direct macrophage polarization toward M2 phenotype (Wang et al. 2017), and subsequently TNF-α, which belongs to cytokines of M1 phenotype, may be reduced. Because TNF-α induces osteoclast formation and promotes RANKL expression in stromal cells, our results suggest that the *in vivo* inhibition of LPS-induced osteoclast formation by exendin-4 may be the result of inhibition of LPS-induced TNF-α expression in macrophages, and subsequent suppression of RANKL expression in stromal cells.

GLP-1 receptors are widely expressed in the body, including osteoclasts, osteocytes, and osteoblasts (Pereira et al. 2015). The effects of GLP-1 receptor agonists on bone metabolism have been widely explored recently.

As the rate of orthodontic tooth movement is also closely related to turnover rate of alveolar bone (Verna et al. 2000), this study was performed to investigate the effect of GLP-1 receptor agonist on orthodontic tooth movement.

GLP-1 receptor deficient mice were reported to have osteopenia and increased osteoclast formation (Yamada et al. 2008, Mieczkowska et al. 2015), suggesting that the GLP-1 signaling pathway had an anti-resorptive effect on bone metabolism. Exendin-4 has been reported for its positive effect on the bone density of diabetes-induced, ovariectomy (OVX)-induced, and high fat diet-induced osteoporotic rodent models (Ma et al. 2013, Pereira et al. 2017, Nuche-Berenguer et al. 2011, Mansur et al. 2019). Most previous literatures indicated that exendin-4 indirectly inhibit osteoclastogenesis of rodents possibly through increasing OPG/RANKL ratio (Nuche-Berenguer et al. 2009, Nuche-Berenguer et al. 2011, Ma et al. 2013), decreasing TNF-α expression (Shen et al. 2018) in the bone

tissue, or reducing serum calcitonin level (Pereira et al. 2015). Direct effect of exendin-4 through activation of GLP-1 receptors on osteoclasts may not be the possible mechanism as evidenced by little or no *in vitro* effects (Pereira et al. 2015, Shen et al. 2018). A previous ovariectomized rat study showed that subcutaneous injections of exendin-4 increased the serum levels of bone formation markers, such as alkaline phosphatase, osteocalcin, and N-terminal propeptide of type 1 procollagen, and increased *in vivo* osteoblast number (Ma et al. 2013). Moreover, exendin-4 promotes the differentiation of bone marrow stromal cells into osteoblasts instead of adipocytes by synergizing with Wnt signaling pathway (Meng et al. 2016). In the alveolar bone, exendin-4 also regulates Wnt and NF-κB signaling in the osteogenic differentiation of periodontal stem cells under inflammatory condition (Liu et al. 2019). Therefore, exendin-4 can down-regulate bone resorption and up-regulate bone formation.

Administrations of medicines or cytokines that can inhibit osteoclasts

have been found to be associated with decreased orthodontic tooth movement (Kitaura et al. 2008, Fujimura et al. 2009, Yoshimatsu et al. 2012, Zaki et al. 2015). In this study, we found diabetic medicine exednin-4 inhibited orthodontic tooth movement at a very high dose. Previous rodent studies have shown that long-term subcutaneous injections of low-dose exendin-4 (equal or less than 0.2 μg/day) improved OVX-induced osteoporosis. However, there is no significant change of orthodontic tooth movement in the 0.2 μg and 4 μg group possibly due to short-term injections in the present study. Therapeutic doses of exendin-4 for diabetic patients, which are as low as the dose in 0.2 μg group, are difficult to significantly affect orthodontic tooth movement in the short term. According to our previous works, short-term injections of high-dose exendin-4 (20μg) were capable of ameliorating LPS-induced bone resorption and osteoclast formation on the murine calvariae (Shen et al. 2018). Although inflammation-induced by orthodontic tooth movement is

not as severe as that induced by LPS, inhibition of orthodontic tooth movement may still requires high-dose exendin-4. Low sample size in each group and poor distribution of exendin-4 in the alveolar bone after local injections may also be the possible contributors.

Root resorption is an inevitable phenomenon of orthodontic treatment, especially in clinical cases with elongated treatment duration, heavy mechanical loading, and hormone unbalance, and high gene susceptibility (Lopatiene et al 2008). In this study, severe root resorption was seen in PBS group because of constant heavy loading force. However, high-dose exendin-4 potently prevented this severe root resorption, which indicates activation of GLP-1 receptors may play an important role during orthodontic root resorption.

Exendin-4 inhibits expression of TNF-α through inhibiting NF-kB pathway (Lee et al. 2016). Macrophage polarization is also directed toward M2 phenotype by exendin-4, and subsequently TNF-α belonging to

cytokines of M1 phenotype are reduced (Wang et al. 2017). It was reported that subcutaneous administrations of exendin-4 for 3 months reduced RANKL expression, increased OPG expression, and reduced RANKL/OPG ratio of ovariectomized rats (Ma et al. 2013). OPG is an inhibitor of osteoclasts and orthodontic tooth movement (Kanzaki et al. 2004). Although increased slightly in the exendin-4 group, OPG mRNA expression wasn't significantly affected by exendin-4 in this study. Further study with longer administration duration is required to ascertain the effect of exendin-4 on OPG expression during orthodontic tooth movement.

It has been reported that exendin-4 still improved the blood glucose control of wild-type mice without affecting the serum insulin level (Fan et al. 2011). Moreover, mice in our high-dose group still tolerate exendin-4 until the final day of orthodontic tooth movement. Thus, high-dose injections of exendin-4 are acceptable for wild-type mice without any significant adverse effects. The effect of diabetes mellitus on orthodontic

tooth movement is still not understood, because controversial results were shown in different rodent studies (Plut et al. 2015, Braga et al. 2011, Arita et al. 2016). Nevertheless, decreased bone turnover rate of diabetic patients may be an important concern during orthodontic treatment (Verhaeghe et al. 1990). Further experiments investigating the role of exendin-4 in orthodontic tooth movement of diabetic mice are still warranted.

6. Conclusions

In conclusion, our results suggested that exendin-4 can inhibit LPS-induced osteoclast formation and bone resorption *in vivo*. The underlying mechanism may be related to its inhibition in the production of LPS-induced TNF-α in macrophages, but not related to its direct effect on osteoclast precursors or RANKL expression in stromal cells. Exendin-4 inhibits osteoclast formation and tooth movement during mechanical loading of orthodontic force, so more attention should be paid to orthodontic patients who take exendin-4 for diabetes treatment. Since exendin-4 prevents orthodontic root resorption, GLP-1 receptor may be a treatment target for clinical cases with severe root resorption.

7. References

Abu-Amer Y, Ross FP, Edwards J, Teitelbaum SL (1997) Lipopolysaccharide-stimulated osteoclastogenesis is mediated by tumor necrosis factor via its P55 receptor, *J Clin Invest*, 100(6): 1557-1565.

Arakawa M, Ebato C, Mita T, Hirose T, Kawamori R, Fujitani Y (2009) Effects of exendin-4 on glucose tolerance, insulin secretion, and beta-cell proliferation depend on treatment dose, treatment duration and meal contents. *Bioch Biophy Res Commun* 390:809–814.

Arakawa M, Mita T, Azuma K, Ebato C, Goto H, Nomiyama T, Fujitani Y, Hirose T, Kawamori R, Watada H (2010) Inhibition of monocyte adhesion to endothelial cells and attenuation of atherosclerotic lesion by a glucagon-like peptide-1 receptor agonist, exendin-4. *Diabetes* 59(4):1030-7.

Arita K, Hotokezaka H, Hashimoto M, Nakano-Tajima T, Kurohama T, Kondo T, Darendeliler MA, Yoshida N (2016) Effects of diabetes on tooth movement and root resorption after orthodontic force application in rats. *Orthod Craniofac. Res*19:83–92.

Aronoff DM, Canetti C, Serezani CH, Luo M, Peters-Golden M (2005) Cutting edge: macrophage inhibition by cyclic AMP (cAMP): differential roles of protein kinase A and exchange protein directly activated by cAMP-1. *J Immunol* 174: 595–599.

Aubert RE, Herrera V, Chen W, Haffner SM, Pendergrass M (2010) Rosiglitazone and pioglitazone increase fracture risk in women and men with type 2 diabetes, *Diabetes Obes Metab*, 12(8): 716-721.

Azuma Y, Kaji K, Katogi R, Takeshita S, Kudo A (2000) Tumor necrosis factor-alpha induces differentiation of and bone resorption by osteoclasts, *J Biol Chem* 275(7): 4858-4864.

Bazelier MT, Gallagher AM, van Staa TP, Cooper C, Leufkens HG, Vestergaard P, de Vries F (2012) Use of thiazolidinediones and risk of osteoporotic fracture: disease or drugs?, *Pharmacoepidemiol Drug Saf*, 21(5): 507-514.

Bazelier MT, Vestergaard P, Gallagher AM, van Staa TP, Cooper C, Leufkens HG, de Vries F (2012) Risk of fracture with thiazolidinediones: disease or drugs?, *Calcif Tissue Int* 90(6): 450-457.

Betteridge DJ (2011) Thiazolidinediones and fracture risk in patients with

Type 2 diabetes, *Diabet Med* 28(7): 759-771.

Bilezikian JP, Josse RG, Eastell R, Lewiecki EM, Miller CG, Wooddell M, Northcutt AR, Kravitz BG, Paul G, Cobitz AR, Nino AJ, Fitzpatrick LA (2013) Rosiglitazone decreases bone mineral density and increases bone turnover in postmenopausal women with type 2 diabetes mellitus, *J Clin Endocrinol Metab*, 98(4): 1519-1528.

Bostanci N, Allaker RP, Belibasakis GN, Rangarajan M, Curtis MA, Hughes FJ, McKay IJ (2007) Porphyromonas gingivalis antagonises Campylobacter rectus induced cytokine production by human monocytes, *Cytokine*, 39(2): 147-156.

Braga SMG., Taddei SRA, Andrade I., Queiroz-Junior CM, Garlet GP,

Repeke CE, Teixeira MM, da Silva TA (2011) Effect of diabetes on orthodontic tooth movement in a mouse model. *Eur. J. Oral Sci* 119:7–14.

Brubaker PL(2007), Incretin-based therapies: mimetics versus protease inhibitors, *Trends Endocrinol Metab*, 18(6): 240-245.

Cao YY, Chen ZW, Gao YH (2015) Exenatide reduces tumor necrosis factor-α-induced apoptosis in cardiomyocytes by alleviating mitochondrial dysfunction. *Chin Med J (Engl)* 128(23):3211–3218.

Chiang CY, Kyritsis G, Graves DT, Amar S (1999) Interleukin-1 and tumor necrosis factor activities partially account for calvarial bone resorption induced by local injection of lipopolysaccharide, *Infect Immun*, 67(8), 4231-4236.

Chung YH, Chang EJ, Kim SJ, Kim HH, Kim HM, Lee SB, Ko JS (2006) Lipopolysaccharide from Prevotella nigrescens stimulates osteoclastogenesis in cocultures of bone marrow mononuclear cells and primary osteoblasts, *J Periodontal Res*, 41(4): 288-296.

Dorecka M, Siemianowicz K, Francuz T (2013). Exendin-4 and GLP-1 decreases induced expression of ICAM-1, VCAM-1 and RAGE in human retinal pigment epithelial cells. *Pharmacol Rep* 65(4):884–890.

Drucker DJ (2003) Glucagon-like peptide-1 and the islet beta-cell: Augmentation of cell proliferation and inhibition of apoptosis. *Endocrinology* 144:5145–5148.

Dumitrescu AL, Abd-El-Aleem S, Morales-Aza B, Donaldson LF (2004) A model of periodontitis in the rat: effect of lipopolysaccharide on bone

resorption, osteoclast activity, and local peptidergic innervation, *J Clin Periodontol*, 31(8): 596-603.

Fan R, Kang Z, He L, Chan J, Xu G (2011) Exendin-4 Improves Blood Glucose Control in Both Young and Aging Normal Non-Diabetic Mice, Possible Contribution of Beta Cell Independent Effects. *PLoS One* 6(5):e20443.

Fujimura Y, Kitaura H, Yoshimatsu M, Eguchi T, Kohara H, Morita Y (2009) Influence of bisphosphonates on orthodontic tooth movement in mice. E*ur J Orthod*31(6):572–577.

Fuller K, Murphy C, Kirstein B, Fox SW, Chambers TJ (2002), TNFalpha potently activates osteoclasts, through a direct action independent of and strongly synergistic with RANKL, *Endocrinology* 143(3):1108-1118.

Garber AJ (2011) Long-acting glucagon-like peptide 1 receptor agonists. A review of their efficacy and tolerability. *Diabetes Care* 34(suppl 2):S279–84.

Garczorz W, Gallego-Colon E, Kosowska A (2018) Exenatide exhibits anti-inflammatory properties and modulates endothelial response to tumor necrosis factor α-mediated activation. *Cardiovasc Ther* 36:1755-5922

Garlet GP, Cardoso CR, Silva TA, B. R. Ferreira, M. J. Avila-Campos, F. Q. Cunha and J. S. Silva (2006), Cytokine pattern determines the progression of experimental periodontal disease induced by Actinobacillus actinomycetemcomitans through the modulation of MMPs, RANKL, and their physiological inhibitors, *Oral Microbiol Immunol*, 21(1), 12-20.

Hakami Z, Kitaura H, Kimura K, Ishida M, Sugisawa H, Ida H (2015) Effect of interleukin-4 on orthodontic tooth movement and associated root resorption. *Eur J Orthod* 37(1):87–94.

Holst JJ (2007) The physiology of glucagon-like peptide 1, *Physiol Rev*, 87(4): 1409-1439.

Kanzaki H., Chiba M., Takahashi I., Haruyama N., Nishimura M., Mitani H. Local OPG gene transfer to periodontal tissue inhibits orthodontic tooth movement. J. Dent. Res. 2004;83:920–925.

Kikuchi T, Matsuguchi T, Tsuboi N, Mitani A, Tanaka S, Matsuoka M, Yamamoto G, Hishikawa T, Noguchi T, Yoshikai Y (2001) Gene expression of osteoclast differentiation factor is induced by lipopolysaccharide in mouse osteoblasts via Toll-like receptors, *J Immunol*, 166(5): 3574-3579.

Kimura K, Kitaura H, Fujii T, Hakami ZW, Takano-Yamamoto T (2012) Anti-c-Fms antibody inhibits lipopolysaccharide-induced osteoclastogenesis in vivo, *FEMS Immunol Med Microbiol*, vol. 64(2): 219-227.

Kitaura H, Kimura K, Ishida M, Kohara H, Yoshimatsu M, Takano-Yamamoto T (2013) Immunological reaction in TNF-alpha-mediated osteoclast formation and bone resorption in vitro and in vivo, *Clin Dev Immunol*, 2013: 181849.

Kitaura H, Sands MS, Aya K, Zhou P, Hirayama T, Uthgenannt B, Wei S, Takeshita S, Novack DV, Silva MJ, Abu-Amer Y, Ross FP, Teitelbaum SL (2004) Marrow stromal cells and osteoclast precursors differentially

contribute to TNF-alpha-induced osteoclastogenesis in vivo, *J Immunol*, 173(8)4838-4846.

Kitaura H, Yoshimatsu M, Fujimura Y, Eguchi T, Kohara H, Yamaguchi A (2008) An anti-c-Fms antibody inhibits orthodontic tooth movement. *J Dent Res* 87(4):396–400.

Kitaura H, Zhou P, Kim HJ, Novack DV, Ross FP, Teitelbaum SL (2005) M-CSF mediates TNF-induced inflammatory osteolysis, *J Clin Invest*, 115(12): 3418-3427.

Kobayashi K, Takahashi N, Jimi E, Udagawa N, Takami M, Kotake S, Nakagawa N, Kinosaki M, Yamaguchi K, Shima N, Yasuda H, Morinaga T, Higashio K, Martin TJ, Suda T (2000) Tumor necrosis factor alpha stimulates osteoclast differentiation by a mechanism independent of the

ODF/RANKL-RANK interaction, *J Exp Med* 191(2): 275-286.

Korner M, Stockli M, Waser B, Reubi JC (2007) GLP-1 receptor expression in human tumors and human normal tissues: potential for in vivo targeting. *Journal of Nuclear Medicine* 48:736–743.

Lee YS, Jun HS (2016) Anti-Inflammatory Effects of GLP-1-Based Therapies beyond Glucose Control. *Mediat Inflamm* 2016:3094642.

Liu H, Zheng J, Zheng T, Wang P (2019) Exendin-4 regulates Wnt and NF-κB signaling in lipopolysaccharide-induced human periodontal ligament stem cells to promote osteogenic differentiation. *Int Immunopharmacol* 75:105801.

Loke YK, Singh S, Furberg CD (2009) Long-term use of thiazolidinediones

and fractures in type 2 diabetes: a meta-analysis, *CMAJ*, 180(1): 32-39.

Lopatiene K, Dumbravaite A (2008) Risk factors of root resorption after orthodontic treatment. *Stomatologija* 10(3):89–95.

Ma X, Hui H, Liu Z, He G, Hu J, Meng J, Guan L, Luo X (2009) Poly-GLP-1, a novel long-lasting glucagon-like peptide-1 polymer, ameliorates hyperglycaemia by improving insulin sensitivity and increasing pancreatic beta-cell proliferation, *Diabetes Obes Metab*, 11(10): 953-965.

Ma X, Meng J, Jia M, Bi L, Zhou Y, Wang Y, Hu J, He G, Luo X (2013) Exendin-4, a glucagon-like peptide-1 receptor agonist, prevents osteopenia by promoting bone formation and suppressing bone resorption in aged ovariectomized rats, *J Bone Miner Res*, 28(7):1641-1652.

Mabilleau G, Mieczkowska A, Chappard D (2014) Use of glucagon-like

peptide-1 receptor agonists and bone fractures: a meta-analysis of randomized clinical trials, *J Diabetes*, 6(3): 260-266.

Mansur SA, Mieczkowska A, Flatt PR, Chappard D, Irwin N, Mabilleau G (2019) The GLP-1 receptor agonist exenatide ameliorates bone composition and tissue material properties in high fat fed diabetic mice. *Front Endocrinol* 10:51.

Meier JJ, Nauck MA, Kranz D, Holst JJ, Deacon CF, Gaeckler D, Schmidt WE, Gallwitz B (2004) Secretion, degradation, and elimination of glucagon-like peptide 1 and gastric inhibitory polypeptide in patients with chronic renal insufficiency and healthy control subjects, *Diabetes*, vol. 53(3): 654-662.

Meng J, Ma X, Wang N, Jia M, Bi L, Wang Y (2016) Activation of GLP-1

Receptor Promotes Bone Marrow Stromal Cell Osteogenic Differentiation through beta-Catenin. *Stem Cell Reports* 6:633.

Mieczkowska A, Irwin N, Flatt PR, Chappard D, Mabilleau G (2013) Glucose-dependent insulinotropic polypeptide (GIP) receptor deletion leads to reduced bone strength and quality. *Bone* 56:337–342.

Moayer A, Mohamadpour M, Mousavi SF, Shirzadpour E, Mohamadpour S, Amraei M (2017) Fracture risk in patients with type 2 diabetes mellitus and possible risk factors: a systematic review and meta-analysis, *Ther Clin Risk Manag* 13:455-468.

Montagnani A, Gonnelli S (2013) Antidiabetic therapy effects on bone metabolism and fracture risk, *Diabetes Obes Metab*, 15 (9):784-791, 2013.

Mormann M, Thederan M, Nackchbandi I, Giese T, Wagner C, Hansch GM (2008) Lipopolysaccharides (LPS) induce the differentiation of human monocytes to osteoclasts in a tumour necrosis factor (TNF) alpha-dependent manner: a link between infection and pathological bone resorption, *Mol Immunol*, 45(12), 3330-3337.

Nielsen LL, Baron AD (2003) Pharmacology of exenatide (synthetic exendin-4) for the treatment of type 2 diabetes, *Curr Opin Investig Drugs*, 4(4): 401-405.

Nuche-Berenguer B, Lozano D, Gutierrez-Rojas I, Moreno P, Mariñoso ML, Esbrit P, Villanueva-Peñacarrillo ML (2011) GLP-1 and exendin-4 can reverse hyperlipidic-related osteopenia. *J Endocrinol* 209:203–210.

Nuche-Berenguer B, Moreno P, Esbrit P, Dapia S, Caeiro JR, Cancelas J,

Haro-Mora JJ, Villanueva-Penacarrillo ML (2009) Effect of GLP-1 treatment on bone turnover in normal, type 2 diabetic, and insulin-resistant states, *Calcif Tissue Int*, 84(6): 453-461.

Nuche-Berenguer B, Moreno P, Portal-Nunez S, Dapia S, Esbrit P, Villanueva-Penacarrillo ML (2010) Exendin-4 exerts osteogenic actions in insulin-resistant and type 2 diabetic states, *Regul Pept*, 159(1-3): 61-66.

Ogawa S Kitaura H, Kishikawa A, Qi J, Shen WR, Ohori F, Noguchi T, Marahleh A, Nara Y, Ochi Y, Mizoguchi I. (2019). TNF-α is responsible for the contribution of stromal cells to osteoclast and odontoclast formation during orthodontic tooth movement. *PLoS One* 14(10): e0223989.

Orcel P, Feuga M, Bielakoff J, De Vernejoul MC (1993) Local bone injections of LPS and M-CSF increase bone resorption by different

pathways in vivo in rats, *Am J Physiol*, 264(3): 391-397.

Pereira M, Gohin S, Roux JP, Fisher A, Cleasby ME, Mabilleau G (2017) Exenatide Improves Bone Quality in a Murine Model of Genetically Inherited Type 2 Diabetes Mellitus. *Front Endocrinol* 8:327.

Pereira M, Jeyabalan J, Jørgensen CS (2015) Chronic administration of glucagon-like peptide-1 receptor agonists improves trabecular bone mass and architecture in ovariectomised mice. *Bone* 81:459-67.

Pereira M, Jeyabalan J, Jorgensen CS, Hopkinson M, Al-Jazzar A, Roux JP, Chavassieux P, Orriss IR, Cleasby ME, Chenu C (2015) Chronic administration of Glucagon-like peptide-1 receptor agonists improves trabecular bone mass and architecture in ovariectomised mice, *Bone*, 81: 459-467.

Plut A, Sprogar Š, Drevenšek G (2015). Bone remodeling during orthodontic tooth movement in rats with type 2 diabetes. *Am J Orthod Dentofacial Orthop*148:1017-1025.

Redlich K, Hayer S, Ricci R, David JP, Tohidast-Akrad M, Kollias G, Steiner G, Smolen JS, Wagner EF, Schett G (2002) Osteoclasts are essential for TNF-alpha-mediated joint destruction, *J Clin Invest* 110(10): 1419-1427.

Saeed J, Kitaura H, Kimura K, Ishida M, Sugisawa H, Ochi Y, Kishikawa A, Takano-Yamamoto T (2016) IL-37 inhibits lipopolysaccharide-induced osteoclast formation and bone resorption in vivo, *Immunol Lett*, 175: 8-15.

Sakuma Y, Tanaka K, Suda　M, Yasoda A, Natsui K, Tanaka I, Ushikubi F, Narumiya S, Segi E, Sugimoto Y, Ichikawa A, Nakao K (2000) Crucial involvement of the EP4 subtype of prostaglandin E receptor in osteoclast formation by proinflammatory cytokines and lipopolysaccharide, *J Bone Miner Res*, 15(2): 218-227.

Schwartz AV, Vittinghoff E, Bauer DC, Hillier TC, Strotmeyer ES, Ensrud KE, Donaldson MG, Cauley JA, Harris TB, Koster A, Womack CR, Palermo L, Black DM (2011) Study of Osteoporotic Fractures Research, G. Osteoporotic Fractures in Men Research, A. Health and G. Body Composition Research, Association of BMD and FRAX score with risk of fracture in older adults with type 2 diabetes, *JAMA* 305(21): 2184-2192.

Shen WR, Kimura K, Ishida M, Sugisawa H, Kishikawa A, Shima K, Ogawa S, Qi J, Kitaura H (2018) The glucagon-like Peptide-1 receptor

agonist Exendin-4 inhibits lipopolysaccharide-induced osteoclast formation and bone resorption via inhibition of TNF-α expression in macrophages. *J Immunol Res* 2018:5783639.

Teitelbaum SL (2000) Bone resorption by osteoclasts, *Science* 289(5484):1504-1508.

Teitelbaum SL (2007) Osteoclasts: what do they do and how do they do it? *Am J Pathol*170(2): 427-435.

Tyrovola JB, Spyropoulos MN, Makou M, Perrea D (2008) Root resorption and the OPG/RANKL/RANK system: A mini review. *J Oral Sci* 50:367–76.

Verna C, Dalstra M, Melsen B (2000) The rate and the type of orthodontic

tooth movement is influenced by bone turnover in a rat model. *Eur J Orthod* 22:343–52.

Verhaeghe J, Van Herck E, Visser WJ, Suiker AM, Thomasset M, Einhorn TA, Faierman E, Bouillon R (1990) Bone and mineral metabolism in BB rats with long-term diabetes: decreased bone turnover and osteoporosis. *Diabetes* 39:477–482.

Vestergaard P, Rejnmark L, Mosekilde L (2005) Relative fracture risk in patients with diabetes mellitus, and the impact of insulin and oral antidiabetic medication on relative fracture risk, *Diabetologia* 48(7): 1292-1299.

Wada N, Maeda H, Yoshimine Y, Akamine A (2004) Lipopolysaccharide stimulates expression of osteoprotegerin and receptor activator of

NF-kappa B ligand in periodontal ligament fibroblasts through the induction of interleukin-1 beta and tumor necrosis factor-alpha, *Bone*, vol. 35(3), 3: 629-635.

Walsh JS, Vilaca T (2017) Obesity, Type 2 Diabetes and Bone in Adults, *Calcif Tissue Int* 100(5): 528-535.

Wang N, Gao J, Jia M, Ma X, Lei Z, Da F, Yan F, Zhang H, Zhou Y, Li M (2017) Exendin-4 induces bone marrow stromal cells migration through bone marrow-derived macrophages polarization via PKA-STAT3 signaling pathway. *Cell Physiol Biochem* 44(5):1696-1714.

Wei Q, Sun YQ, Zhang J (2012) Exendin-4, a glucagon-like peptide-1 receptor agonist, inhibits cell apoptosis induced by lipotoxicity in pancreatic *β*-cell line. *Peptides* 37(1):18–24.

World Health Organization (2016) *Global Report on Diabetes* 2016: 20-33.

Yamada C, Yamada Y, Tsukiyama K, Yamada K, Udagawa N, Takahashi N, Tanaka K, Drucker DJ, Seino Y, Inagaki N (2008) The murine glucagon-like peptide-1 receptor is essential for control of bone resorption, *Endocrinology*, 149(2): 574-579.

Yamada C, Yamada Y, Tsukiyama K, Yamada K, Udagawa N, Takahashi N (2008) The murine glucagon-like peptide-1 receptor is essential for control of bone resorption. *Endocrinol*149:574–579.

Yang CY, Jeon HH, Alshabab A (2018) RANKL deletion in periodontal ligament and bone lining cells blocks orthodontic tooth movement. *Intl J Oral Sci* 10(1):31–39.

Yoshimatsu M, Kitaura H, Fujimura Y, Kohara H, Morita Y, Eguchi T (2012). Inhibitory effects of IL-12 on experimental tooth movement and root resorption in mice. *Arch. Oral Biol* 57: 36–43.

Zhang YS, Weng WY, Xie BC, Meng Y, Hao YH, Liang YM, Zhou ZK (2018) Glucagon-like peptide-1 receptor agonists and fracture risk: a network meta-analysis of randomized clinical trials. *Osteoporos. Int* 29:2639–2644.

Zou W, Bar-Shavit Z (2002) Dual modulation of osteoclast differentiation by lipopolysaccharide, *J Bone Miner Res*, 17(7): 1211-1218

8. Figure legends and figures

Figure 1

In vivo effect of exendin-4 on lipopolysaccharide (LPS)-induced osteoclast formation.

(A) Histological sections of mouse calvariae after 5-day daily supracalvarial injections with phosphate-buffered saline (PBS), LPS (100μg/day), LPS (100μg/day) with exendin-4 (20 μg/day), and exendin-4 (20 μg/day). Tartrate-resistant acid phosphatase (TRAP) staining and haematoxylin counterstaning were performed. TRAP-positive cells were stained dark red. (B) The numbers of TRAP-positive cells in the suture mesenchyme of calvaria from the mouse groups administered with PBS, LPS, LPS with exendin-4, and exendin-4, respectively. Data is expressed as means ± standard deviation (SD). Statistical significance were determined by the Scheffe's test ($n = 4$; $^{**}p < 0.01$).

Figure 2

Exendin-4 inhibited LPS-induced bone resorption *in vivo*.

(A) 3D reconstructed images of calvariae from micro-CT scanning. Mice were subjected to 5-day daily subcutaneous injections on the calvariae with PBS, LPS (100 μg/day) with or without exendin-4 (20 μg/day), and exendin-4 (20 μg/day), and calvariae were excised on the sixth day. The red dots indicate areas of bony destruction. (B) Ratio of bone destruction area to total bone area. Data is expressed as means ± SD (n = 4; $^{*}p < 0.05$, $^{**}p < 0.01$). The statistical significance of differences was determined by Scheffe's test. (C) Serum levels of C-terminal telopeptide of type I collagen (CTX) determined by a mouse CTX assay kit. Data is expressed as means ± SD. The statistical significance of differences was determined using the Scheffe's test (n = 4; **p < 0.01).

Figure 3

Exendin-4 suppressed expression of LPS-induced tumor necrosis factor (TNF)-α and receptor activator of NF-kB ligand (RANKL) *in vivo*.

TNF-α and RANKL mRNA levels in mouse calvariae were determined using real-time RT-PCR. Total RNA was isolated from mouse calvariae after 5-day daily supracalvarial injections with PBS, LPS (100 μg/day) with or without exendin-4 (20 μg/day), and exendin-4 alone (20 μg/day). TNF-α and RANKL mRNA levels were normalized to the expression of glyceraldehyde 3-phosphate dehydrogenase (GAPDH). Data is expressed as means ± SD. The statistical significance of differences was determined using the Scheffe's test ($n = 4$; $^{*}p < 0.05$, $^{**}p < 0.01$).

Figure 4

Exendin-4 had no effect on RANKL-induced osteoclast formation, TNF-α-induced osteoclast formation, osteoclast precursor cell viability, or LPS-induced RANKL expression in stromal cells *in vitro*.

(A) Microscopic images and numbers of TRAP-positive cells. Osteoclast precursors were treated with macrophage colony stimulating factor (M-CSF) alone, M-CSF with RANKL, M-CSF with RANKL and exendin-4, and M-CSF with exendin-4 for 5 days, then stained with TRAP solution. (B) Microscopic images and numbers of TRAP-positive cells. Osteoclast precursors were treated with M-CSF alone, M-CSF with TNF-α, M-CSF with TNF-α and exendin-4, and M-CSF with exendin-4 for 5 days, then stained with TRAP solution. (C) Cell viability of osteoclast precursor cells treated with M-CSF alone and M-CSF with exendin-4 for 5 days. Cell viability was determined by cell counting kit-8. Data is presented as percentage activity relative to the activity in the culture with M-CSF alone, and are expressed as means ± SD. (D) RANKL mRNA expression levels in stromal cells determined by real-time RT-PCR method. Total RNA was extracted from stromal cells that were cultured with PBS, LPS with or without exendin-4, and exendin-4 alone, respectively. RANKL mRNA

levels were normalized to that of GAPDH. Statistical significance of differences was determined by Scheffe's test (n = 4; **P < 0.01).

Figure 5

Exendin-4 inhibited LPS-induced expression of TNF-α in macrophages.

TNF-α mRNA levels in macrophages were detected by real-time RT-PCR. Total RNA was isolated from macrophages cultured with PBS, LPS with or without exendin-4, and exendin-4 alone. TNF-α mRNA levels were normalized to the levels of GAPDH. Statistical significance of differences was determined by the Scheffe's test (n = 4; *p < 0.05, **P < 0.01).

Figure 6

Dose-dependent effect of exendin-4 (Ex-4) injections on orthodontic tooth movement on day 12 (A) An intraoral photograph after 12-day orthodontic

tooth movement. A nickel-titanium spring was tied between upper left first molar and anterior alveolar bone. A gap between upper left first (M1) and second molars (M2) can be seen on the final day. (B) The method of measuring orthodontic tooth movement distance on silicone impression. The gap (double arrow) between the distal marginal ridge of the first molar and mesial marginal ridge of the second molar on the line (dash line) connecting the central fossae of the first and second molars was measured by a dissecting microscope. (C) Silicone impressions and tooth movement distances of mice injected with 20 μl solutions of PBS, 0.2 μg, 4 μg, or 20 μg exendin-4 every 2 days (n=4). *$p < 0.05$, **$p < 0.01$

Figure 7

Histological evaluation of osteoclast numbers after 12 days of orthodontic tooth movement. The maxillae injected with PBS or 20 μg exendin-4 were obtained for preparation of histological sections (n=4). Large TRAP (+)

osteoclasts (arrow) appeared on the alveolar bone surface mesial to bucco-lingual root axis (dash line) of distobuccal root of upper left first molar. D: distal; M: mesial; R: root; P: PDL; A, alveolar bone. *$p < 0.05$

Figure 8

Histological evaluation of odontoclast numbers and root resorption surface percentages after 12 days of orthodontic loading (A) TRAP (+) odontoclasts (arrow) resting on root surface were found on the compression side of distobuccal root of upper left first molar in PBS group and 20 μg exendin-4 group (n=4). (B) Thinning or lacunae of cementum with overlying odontoclasts was considered as resorptive root surface (gray dash line). Root resorption surface percentage (%) was calculated by dividing the length of resorption surface by the whole length of root surface on the compression side (intact surface + resorptive surface) D: distal; M: mesial; R: root; P: PDL. *$p < 0.05$

Figure 9

Effect of local exendin-4 (Ex-4) administrations on expressions of RANKL (A), TNF-α (B), and OPG mRNA (C) and RANKL/OPG ratio (D) in the maxillae during orthodontic tooth movement. Maxillae with injections of PBS or 20 μg exendin-4 solutions were excised for RT-PCR analysis after 12 days of orthodontic loading (n=4). *$p < 0.05$ **$p < 0.01$

Figure 1

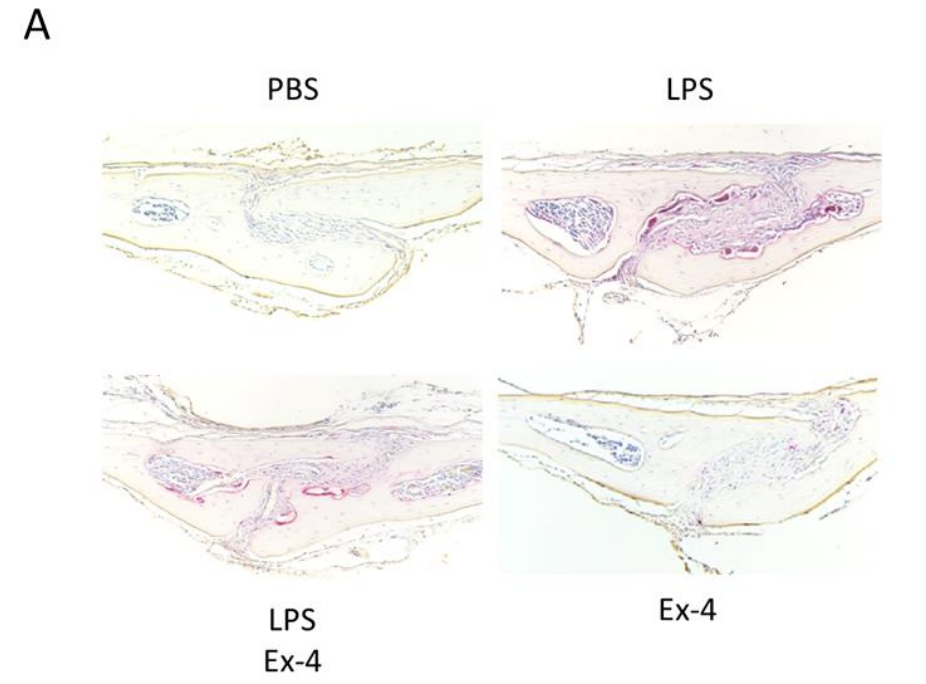
A
PBS
LPS
LPS
Ex-4
Ex-4
B
**
**
**
**
**
Number of TRAP-positive cells
(cell/section)
14
12
10
8
6
4
2
0
PBS
LPS
LPS
Ex-4
Ex-4

Figure 2

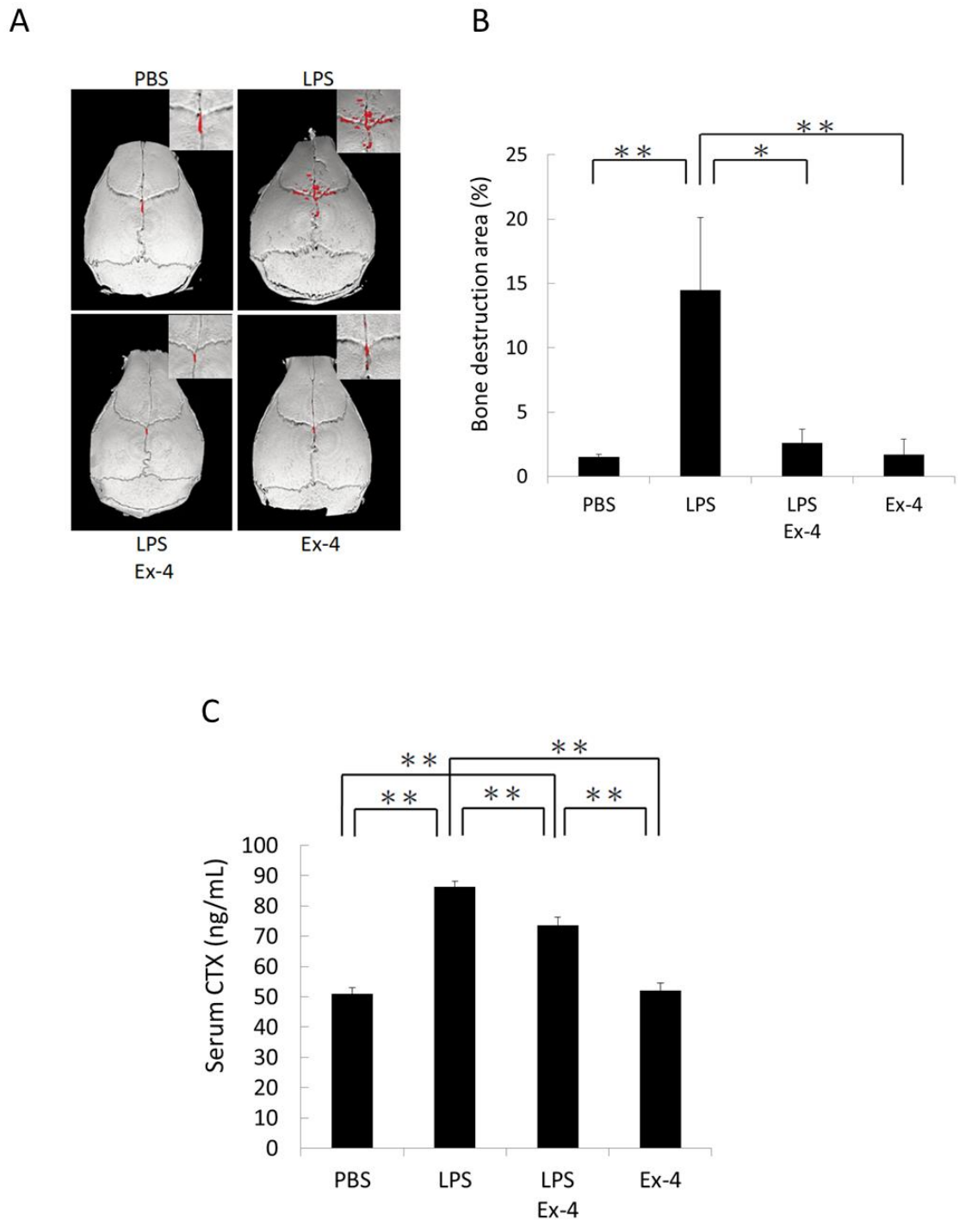
A
PBS
LPS
LPS
Ex-4
Ex-4
B
Bone destruction area (%)
25
20
15
10
5
0
**
*
**
PBS
LPS
LPS
Ex-4
Ex-4
C
Serum CTX (ng/mL)
100
90
80
70
60
50
40
30
20
10
0
**
**
**
**
PBS
LPS
LPS
Ex-4
Ex-4

Figure 3

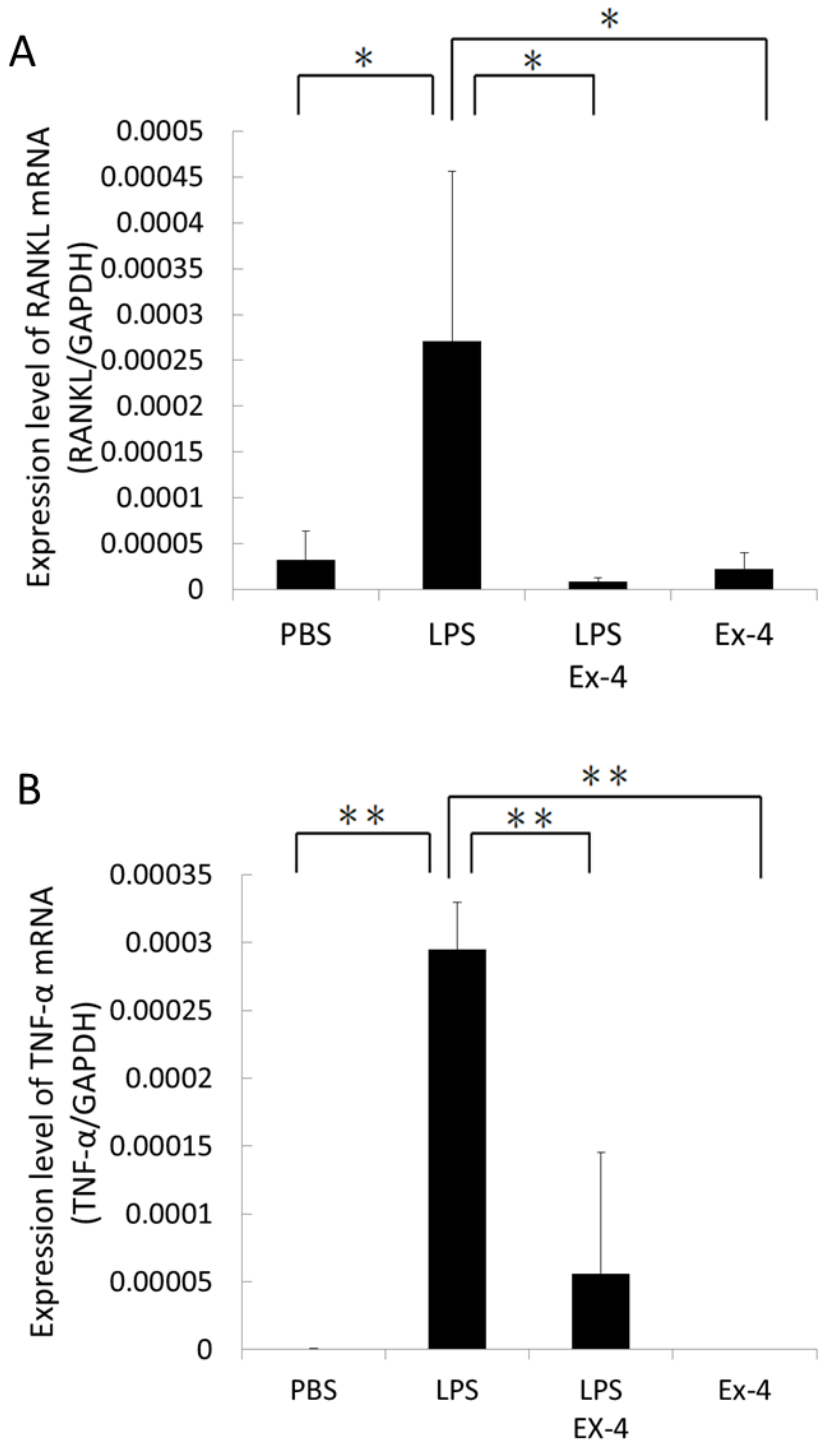
A
*
*
*
Expression level of RANKL mRNA (RANKL/GAPDH)
0.0005
0.00045
0.0004
0.00035
0.0003
0.00025
0.0002
0.00015
0.0001
0.00005
0
PBS
LPS
LPS Ex-4
Ex-4
B
**
**
**
Expression level of TNF-α mRNA (TNF-α/GAPDH)
0.00035
0.0003
0.00025
0.0002
0.00015
0.0001
0.00005
0
PBS
LPS
LPS EX-4
Ex-4

Figure 4

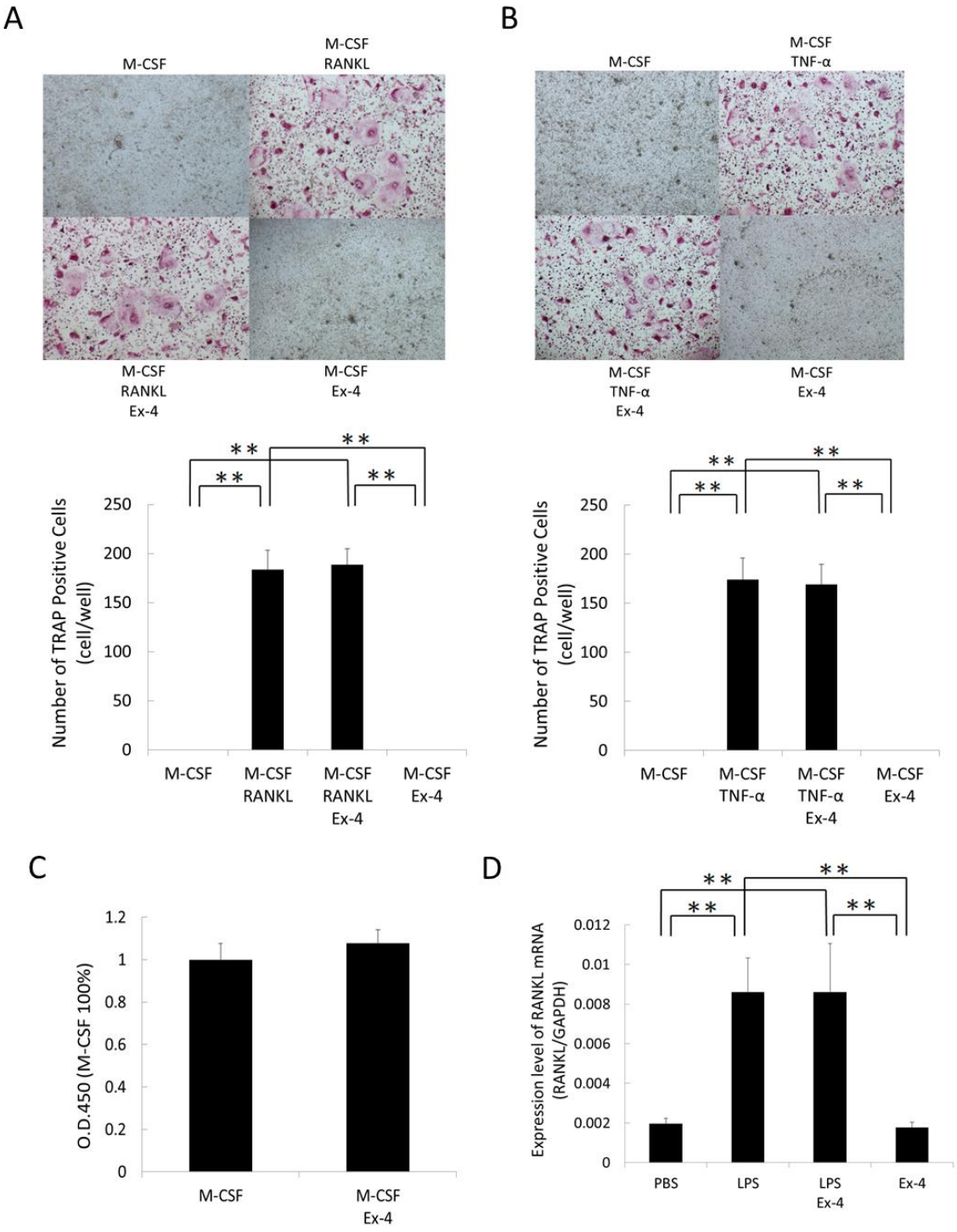
A
M-CSF
M-CSF RANKL
M-CSF RANKL Ex-4
M-CSF Ex-4
Number of TRAP Positive Cells (cell/well)
M-CSF
M-CSF RANKL
M-CSF RANKL Ex-4
M-CSF Ex-4
B
M-CSF
M-CSF TNF-α
M-CSF TNF-α Ex-4
M-CSF Ex-4
Number of TRAP Positive Cells (cell/well)
M-CSF
M-CSF TNF-α
M-CSF TNF-α Ex-4
M-CSF Ex-4
C
O.D.450 (M-CSF 100%)
M-CSF
M-CSF Ex-4
D
Expression level of RANKL mRNA (RANKL/GAPDH)
PBS
LPS
LPS Ex-4
Ex-4

Figure 5

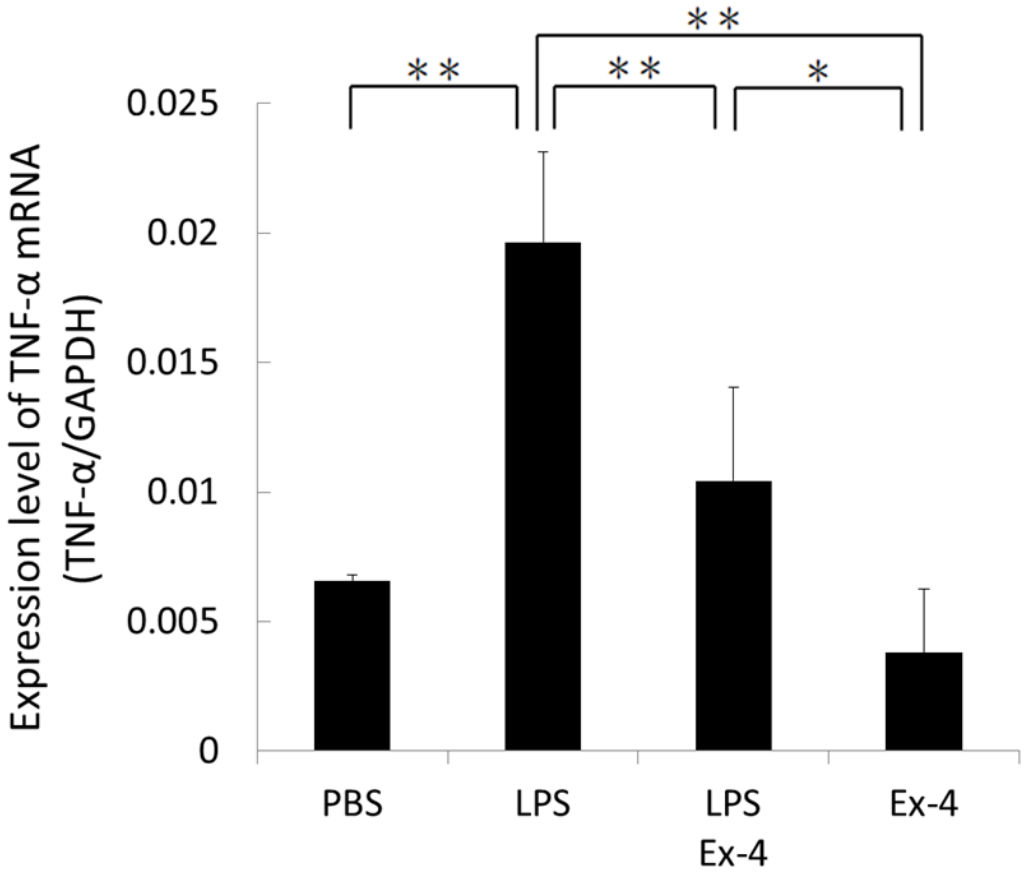
**
**
**
*
Expression level of TNF-α mRNA
(TNF-α/GAPDH)
0.025
0.02
0.015
0.01
0.005
0
PBS
LPS
LPS
Ex-4
Ex-4

Figure 6

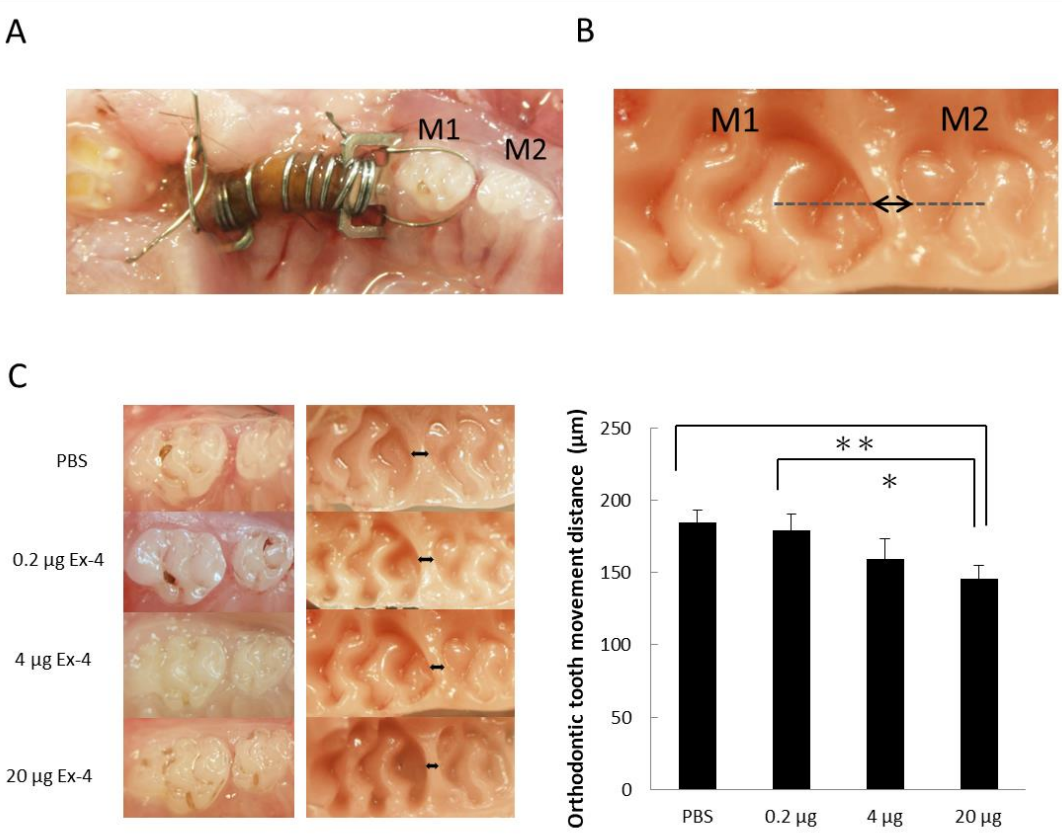
A
M1
M2
B
M1
M2
C
PBS
0.2 μg Ex-4
4 μg Ex-4
20 μg Ex-4
Orthodontic tooth movement distance (μm)
250
200
150
100
50
0
**
*
PBS
0.2 μg
4 μg
20 μg

Figure 7

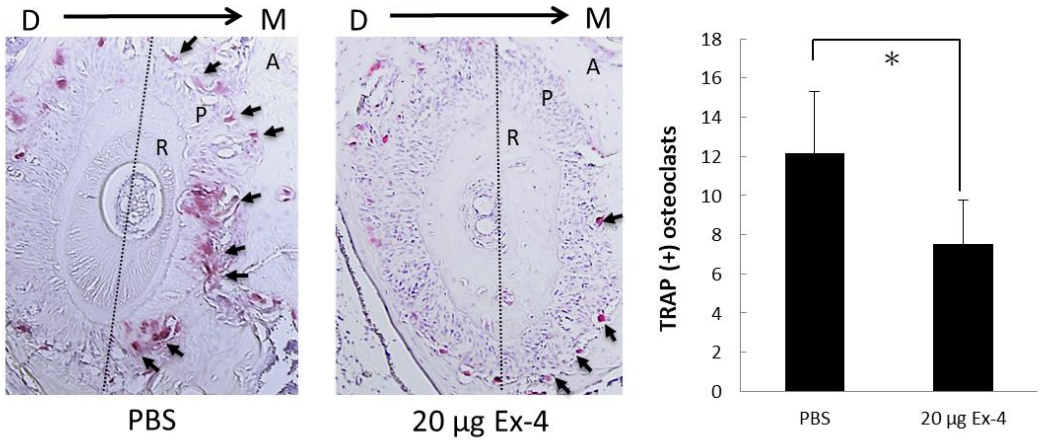
D
M
A
P
R
PBS
D
M
A
P
R
20 µg Ex-4
TRAP (+) osteoclasts
18
16
14
12
10
8
6
4
2
0
*
PBS
20 µg Ex-4

Figure 8

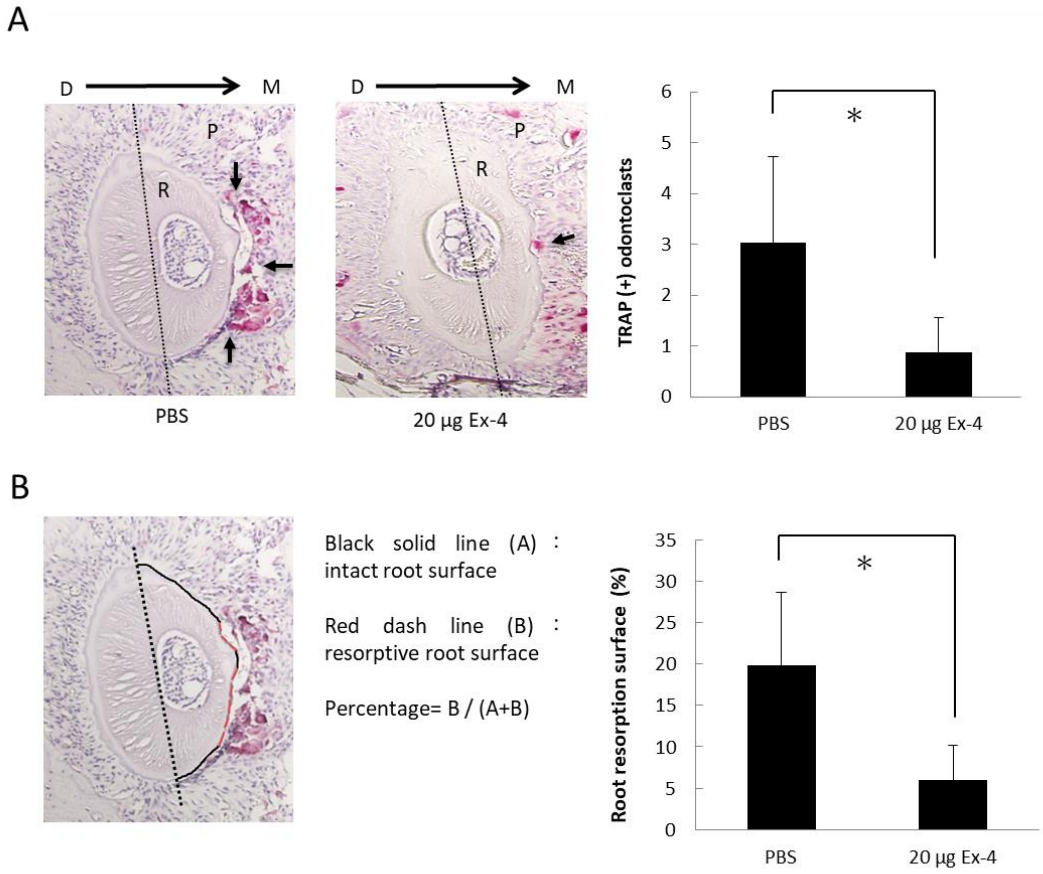
A
D
M
P
R
PBS
20 μg Ex-4
TRAP (+) odontoclasts
0
1
2
3
4
5
6
*
PBS
20 μg Ex-4
B
Black solid line (A) : intact root surface
Red dash line (B) : resorptive root surface
Percentage= B / (A+B)
Root resorption surface (%)
0
5
10
15
20
25
30
35
*
PBS
20 μg Ex-4

Figure 9

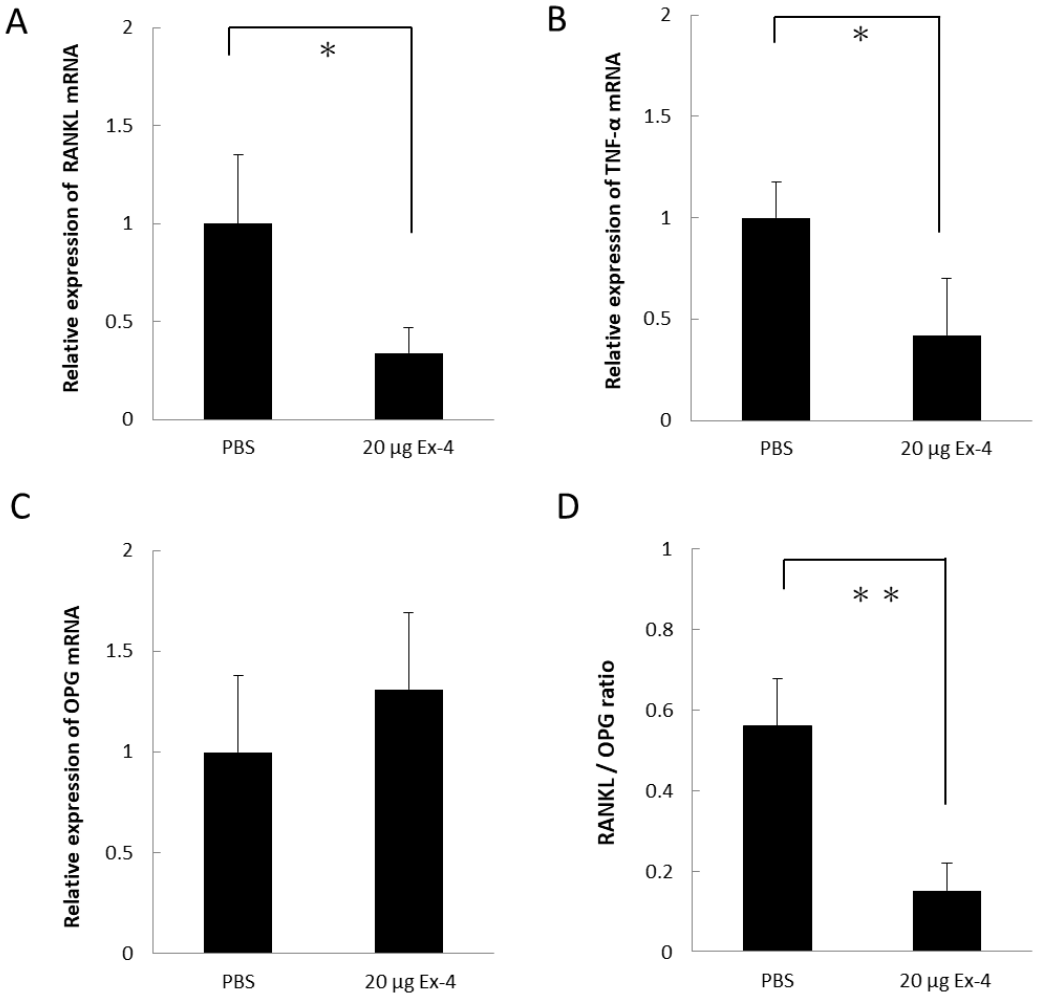
A
Relative expression of RANKL mRNA
2
1.5
1
0.5
0
*
PBS
20 μg Ex-4
B
Relative expression of TNF-α mRNA
2
1.5
1
0.5
0
*
PBS
20 μg Ex-4
C
Relative expression of OPG mRNA
2
1.5
1
0.5
0
PBS
20 μg Ex-4
D
RANKL / OPG ratio
1
0.8
0.6
0.4
0.2
0
* *
PBS
20 μg Ex-4

9. Acknowledgement

Foremost, I would like to express my sincere gratitude to my research supervisors, Dr. Mizoguchi and Dr. Kitaura, for helping me enter this school and finish my research. It was a great honor to work and study under their guidance. I also thank members in my research group for accepting me and arranging things about my experiments. I am extremely grateful for what my department has offered me.

I am extremely grateful to my parents for their love and sacrifices throughout the thirty-three years. My thanks also go to professor Hon and Miss Hurudate for helping me apply scholarship. Even though I failed many times, they still encouraged me and never gave up. I thank Japan-Taiwan exchange association for their scholarship. With it, I can focus on my research instead of worrying economic supplies.